Intermolecular structure in a single component polymer glass: Towards high resolution measurements of the sidechain pair correlation function

A. H. Marcus[a] and M. D. Fayer
Department of Chemistry, Stanford University, Stanford, California 94305

John G. Curro
Sandia National Laboratory, Albuquerque, New Mexico 87185

(Received 10 January 1994; accepted 4 March 1994)

Electronic excitation transport among interacting polymer molecules lightly tagged with chromophore substituents is theoretically examined as a function of tagged polymer concentration in the polymeric solid. The results are compared to experimental data obtained in a previous study [Macromolecules **26**, 3041 (1993)]. The dependence of time-resolved fluorescence observables on intermolecular polymer structure is of primary interest. A theory is presented which describes excitation transport for both donor–donor (DD) and donor–trap (DT) systems. For the case of DD transport, the theory is based on a first order cumulant approximation to the transport master equation. For DT transport, the theory does not involve approximations and is an exact representation of the assumed model. In both cases, the model makes use of the Flory "ideality" postulate by depicting the intramolecular segmental distribution as a Gaussian with a second moment that scales linearly with chain size. The only adjustable parameter in the treatment is the form of the intermolecular segmental pair distribution function $g(r)$. The model is found to be extremely sensitive to the behavior of $g(r)$. Comparisons to experimental data indicate that $g(r)$ is primarily made up of hard core interactions between the chromophore sites. The DT calculations display a higher sensitivity to the form of $g(r)$ than the corresponding DD calculations. For purposes of comparison, the analysis is applied to a DT system in which every polymer chain has chromophore tags. The sensitivity of the method for 100% tagged systems to $g(r)$ is comparable to the analysis for systems with only some of the chains tagged.

I. INTRODUCTION

The elucidation of intermolecular structure in solid polymer glasses and polymer liquids is an unresolved topic that has stimulated numerous theoretical and experimental investigations.[1–13] There are many aspects to this problem. For example, the degree of interpenetration among neighboring polymer coils may be extensive, leading to random packing of the polymer segments.[14] In this case, the intermolecular segmental pair distribution function $g(r)$ which represents the relative probability that segments belonging to two different polymer molecules are separated by the distance r, is a constant (unity) for all separations. Alternatively, certain systems may exhibit behavior where regions near the centers of gravity of Gaussian coils exclude segments belonging to other molecules. In such a situation, the pair distribution function is small for values of r similar to the radius of gyration (R_g), but asymptotically approaches unity as r increases. This deficit in radial distribution probability is referred to in the literature as a correlation hole.[9]

Knowledge of intermolecular polymer structure can be further applied to problems that focus on polymer blend morphology. The structure of nanophase separated domains in polymeric mixtures is not well understood. A nanodomain is a region where the segments of as few as two or three molecules of one component have aggregated. It has been shown that nanodomains exist at temperatures well below the critical point in solid blends which appear macroscopically homogeneous.[15–17] The structure of these domains can directly affect the behavior of the glass transition temperature, since processes responsible for T_g are associated with distance scales comparable to domain size. Independent measurements of T_g and nanodomain structure can therefore establish detailed characteristics such as the critical distance associated with the glass transition.[18]

Kinetic studies of polymer phase transitions can benefit from a detailed analysis of intermolecular structure. Phase separation in miscible polymer blends can be induced by variations in temperature, pressure, or composition. The final, equilibrium state contains different macroscopic regions (phases) dominated by different components of the blend. During the initial and intermediate stages of the phase transition, the structure, local concentration, and size of the nanodomains present must evolve toward the final state. By following the trajectory of the nanodomain structure, new insight can be gained concerning the mechanisms of polymer phase transitions.

In recent years, electronic excitation transfer (EET) studies of chromophores bound to polymers or micelle assemblies has become a useful tool for the elucidation of macromolecular structure.[1,4–8,16,17,19–24] Resonant dipolar coupling between the singlet electronic states of interacting chromophores was first described as a mechanism for EET by Förster.[25,26] The $1/r^6$ dependence of the transition dipole–transition dipole interaction has led to the determination of interchromophore distances which are directly related to the

[a]Present address: The James Franck Institute, The University of Chicago, 5640 S. Ellis, Chicago, IL 60637.

 0021-9606/94/100(12)/9156/14/$6.00

segmental distribution of tagged macromolecules.[6,16,23] This is similar to the role nuclear dipolar relaxation (which also follows a $1/r^6$ dependence) has played in the determination of interatomic distances using nuclear Overhauser enhancement (NOE) studies.[27] The distance effectively sampled by the Förster interaction depends on the oscillator strength of the acceptor chromophore and the spectral overlap between the excited singlet state wave function of the donor and the ground state wave function of the acceptor.[28] This interaction is characterized by the Förster transfer distance R_0. Depending on the specific system, R_0 may range between distances from 6 to 60 Å.[28]

There are two important categories of experimentally accessible EET systems—donor donor and donor trap. Donor–donor (DD) systems involve energy transport among chemically identical chromophores. This means all the chromophores have similar energies such that the excitation can "hop" from site to site. Thus, the trajectory of an initial excitation may follow a complicated pathway among sites before a radiative process (fluorescence) can occur. Donor–trap (DT) systems exhibit direct energy transport between two chemically distinct species. The "donor" chromophore is selectively excited and transfer of the excitation to a "trap" is irreversible. In a DT system, there is no significant back transfer to the donor.

Recently, we have developed analytical methods to describe DD and DT EET among chromophores embedded in spatially complex surfaces.[21] The technique has been applied to DD studies of concentrated micelle suspensions with chromophores restricted to lie at the micelle surfaces,[20] and to pendant chromophores covalently bound to the backbones of polymer chains.[1] For the micelle system, the accuracy of the method has been confirmed by comparison to the results of Monte Carlo simulations.[19] In both experimental situations, EET occurs within a chromophore cluster (e.g., a micelle or a polymer coil) and between clusters.

For DD systems, the method makes use of a truncated cumulant approximation which is based on the assumption that the cumulative effect of all transfer processes is well described by a superposition of pairwise interactions.[29–32] In this way, the multiple step processes which occur in clustered systems may be partitioned into fast events internal to a cluster and the slower transfer steps between interacting clusters. This renormalizes a many-body problem into a tractable two-body problem that can be formulated analytically. Since the interaction between clusters is treated in analogy to the interaction between two "effective chromophores", the technique is called the effective chromophore (EC) method.

The EC method has been successfully applied to experimental DD studies of intermolecular structure in a single component polymer glass [atactic poly(methylmethacrylate)].[1] Measurements of EET among pendant chromophores (2-vinylnaphthalene) randomly tagged to the backbones of polymer coils in low concentration [atactic 6.5% poly(methylmethacrylate-co-2-vinylnaphthalene)] were employed to determine the proximity of segments belonging to other tagged coils. The measurements were performed as a function of tagged copolymer concentration in an untagged polymer host. The analysis of these experiments made use of a theory based on an assumed form for the center-to-center intermolecular radial pair distribution function, $\mathbf{g}_{cm}(R_s)$. Although the analytical theory reproduced the experimental data with a high degree of accuracy, the sensitivity of the calculations to the center-to-center pair distribution was not optimal. In this work, the analysis has been modified to interpret the experimental observables in terms of the segment-to-segment intermolecular radial pair distribution $\mathrm{g}(r)$. The intersegmental $\mathrm{g}(r)$ has the physical meaning of the relative probability of finding two segments on different chains separated by the distance r, averaged over all segment positions, and averaged over all chain configurations.[3] The intersegmental distribution is a more suitable function to characterize interpenetration among chain segments. It is shown below that the experimental observables in both DD and DT systems are extremely sensitive to the functional form of $\mathrm{g}(r)$.

The time-dependent motion of an excitation within an ensemble of interacting chromophores can be characterized by the Green's function solution to the Pauli master equation $G^s(t)$.[33] $G^s(t)$ is the self-part of the Green's function. It represents the probability that the initially excited chromophore is still excited at some later time. Both DD and DT systems are characterized by the behavior of $G^s(t)$. A DD system can involve singlet or triplet excitation transport, while a DT system can also employ electron transfer. For the case of DD transport, the derivation of an analytical expression for $G^s(t)$ requires approximations due to the infinite number of possible excitation pathways. The accuracy of the expression depends on the validity of the approximations. In a DT system, however, the number of excitation pathways are equal to the number of traps and to the probability that a particular pathway occurs is unaffected by another. Consequently, for DT systems, an analytical expression for $G^s(t)$ represents an exact description of the excitation dynamics.

The usefulness of $G^s(t)$ lies in its relationship to the observables obtained from time resolved fluorescence experiments. In the case of energy transfer among chemically identical chromophores (DD transport), $G^s(t)$ is contained in the time dependent fluorescence anisotropy which is given by the time correlation function[34]

$$r(t)=(2/5)\langle P_2[\mu_e(t)\cdot\mu_a(0)]\rangle. \tag{1.1}$$

Here μ_a and μ_e are the unit vectors corresponding to the transition dipoles for absorption of the excitation and emission of the fluorescence, $P_2(x)$ is the second Legendre polynomial, and the angle brackets indicate an ensemble average. $r(t)$ represents the decay of polarization of the fluorescence

$$r(t)=\frac{I_{\parallel}(t)-I_{\perp}(t)}{I_{\parallel}(t)+2I_{\perp}(t)}, \tag{1.2}$$

where $I_{\parallel}(t)$ and $I_{\perp}(t)$ are, respectively, the time dependent polarized fluorescence decays parallel and perpendicular to the polarization of the excitation pulse. A polarized excitation of an ensemble of randomly oriented chromophores results in a polarization-selective initial state. Only chromophores with the appropriate transition dipole directions can be initially excited. Transfer of the excitation to surrounding molecules, which are randomly oriented, and subsequent emission leads to depolarization of the observed

fluorescence. This results in fluorescence anisotropies dominated by the configurational average of the Green's function $\langle G^s(t)\rangle$, provided other depolarization processes (such as chromophore rotation) occur on a slower time scale

$$r(t)\propto\Phi(t)\cdot\langle G^s(t)\rangle \quad \text{(DD)}. \tag{1.3}$$

Here, $\Phi(t)$ represents the rotational contribution to the fluorescence anisotropy.

For the case of DT transport, $\langle G^s(t)\rangle$ represents the nonradiative decay of excitation probability from the ensemble of excited donor chromophores due to excitation or electron transport to traps. In the direct trapping limit, $\langle G^s(t)\rangle$ is proportional to the time dependent decay of the total fluorescence of the excited donor chromophores:

$$I_{\text{tot}}(t)\propto\exp(-t/\tau_F)\cdot\langle G^s(t)\rangle \quad \text{(DT)}, \tag{1.4}$$

where τ_F is the fluorescence lifetime of the donor molecule in the absence of direct trapping processes.

The behavior of DD transport for interacting clusters of chromophores can be understood as a superposition of processes which include both the internal dynamics of a single cluster and the external dynamics among cluster pairs. The decay of $\langle G^s(t)\rangle$ depends on the relative efficiency of competing high frequency transfer processes (those which occur among chromophores in the same cluster) and lower frequency events (transfer between chromophores on different clusters) which increase in frequency and amplitude as the average cluster separation decreases. The limitations in the sensitivity of $r(t)$ to $g(r)$ can be understood in terms of the relative contribution to the fluorescence anisotropy from both intra- and intercluster excitation transfer. The anisotropy of the system of interacting tagged polymers contains a contribution $r_{\text{on}}(t)$ due to the intramolecular EET. Because DD transfer on the initially excited chain can be fast, a detectable change in the total time dependent anisotropy requires a significant component from the concentration dependent chain to chain transport. Therefore, a detailed examination of the interchain structure may be limited by intramolecular transfer processes that compete with the centrally important intermolecular processes.

An alternative method utilizing DT transfer provides an improvement in sensitivity needed to study $g(r)$ in more detail. This is achieved by eliminating the contribution of the intrachain transfer from the experimental observable. The polymer coils are labeled with two different types of chromophores. The first type of chromophore is a donor, while the second type is a trap. The donor is chosen so that its absorption spectrum does not overlap significantly with the absorption spectrum of the trap. After selective excitation of a donor molecule, the excitation may transfer to a trap on another polymer coil, but cannot transfer back to the donor position on the original coil. The donor tagged copolymer has one donor chromophore randomly tagged along the length of the "donor chain," while the trap tagged copolymer has many traps randomly distributed along the "trap chain." Measurements of the time dependent donor fluorescence then contain the necessary information to determine the transfer rates between an excited donor interacting with an ensemble of traps. The transfer dynamics of this DT system involves only contributions from interchain transfer processes. Thus, the fluorescence observable is directly related to the interchain segmental distribution.

This paper is organized in the following manner: In Sec. II, we present the EC method which describes DT and DD excitation transport among tagged guest chains in an untagged (but otherwise identical) host. This formulation of $\langle G^s(t)\rangle$ depends on the intersegmental radial pair distribution function $g(r)$. In Sec. III, the dependence of the transport observables on the functional form of $g(r)$ is discussed. In addition to the clustered chromophore system described by the EC method, an alternative experiment in which every polymer molecule has chromophore tags is introduced. Section IV contains a discussion of the results.

II. ANALYTICAL THEORY OF DT AND DD TRANSFER IN GAUSSIAN POLYMER COILS

In this section, an analytical description of DT and DD transfer among chromophores randomly tagged to the backbones of polymer coils in the amorphous bulk state is presented. The description is based on a model where only some of the polymer coils have chromophore tags. Although this is a nonessential feature for structural studies of one-component systems, such a model is necessary for the development of meaningful descriptions of EET in binary phase separated polymeric blends, which is the subject of a current study.[17] The calculations are based on the positions of the chromophore tags. These positions are assumed to represent a random sampling of the coil segments. The formulation is similar to one previously presented in Ref. 1, however, here the intermolecular polymer structure is properly described by the intercoil site-to-site radial pair distribution function $g(r)$. Additionally, general treatments of DT transfer have been presented elsewhere.[6,19,35] Therefore, only the essential expressions for both DT and DD polymer systems are given here. The reader is referred to the original sources for more details.

A. Microsystem calculations—one donor and $N-1$ traps distributed within two Gaussian surfaces

Consider two identical polymer coils with radius of gyration R_g, separated by the distance R_s. One is designated the "donor coil," while the other is the "trap coil." The donor coil has a single donor chromophore, while the trap coil has $N-1$ traps. On both coils, the chromophores are randomly oriented and distributed along the chain backbones. The intercoil separation R_s may be large, so that the segments of the two molecules do not come into contact, or small so that the segments interpenetrate extensively. We examine the case where the single chromophore on the donor coil is excited and incoherent energy transfer to surrounding traps can occur by a dipole–dipole mechanism.[25,36]

The general expression describing the decay of the donor excited state probability due to excitation transfer for a system of one donor interacting with $N-1$ traps is[35]

$$\langle G^s(t)\rangle = \int_{\mathbf{r}_1} u(\mathbf{r}_1)d\mathbf{r}_1 \int_{\mathbf{r}_2} u(\mathbf{r}_2)\exp[-\omega(\mathbf{r}_{12})t]d\mathbf{r}_2 \times \int_{\mathbf{r}_3} u(\mathbf{r}_3)\exp[-\omega(\mathbf{r}_{13})t]d\mathbf{r}_3 \cdots \int_{\mathbf{r}_N} u(\mathbf{r}_N) \times \exp[-\omega(\mathbf{r}_{1N})t]d\mathbf{r}_N . \quad (2.1)$$

In Eq. (2.1), the donor is labeled by position 1 and the traps by positions $2-N$. For dipolar interactions, the rate constant $\omega(\mathbf{r}_{1i})$ is given by

$$\omega(\mathbf{r}_{1i}) = \frac{1}{\tau_F}\left(\frac{R_0^{\mathrm{DT}}}{r_{1i}}\right)^6 , \quad (2.2)$$

where R_0^{DT} is the critical transfer distance for direct trapping, r_{1i} is the absolute distance between the donor and the ith trap, and τ_F is the fluorescence lifetime of the donor in the absence of traps. The critical transfer distance R_0^{DT} is defined as the distance between an isolated donor–trap pair for which the excitation transfer probability is equal to the probability of deactivation of the donor excited state by fluorescence. Since all of the traps have the same spatial probability distribution used to describe the trap coil's segments, Eq. (2.1) becomes

$$\langle G^s(t)\rangle = \int_{\mathbf{r}_1} u_d(\mathbf{r}_1)d\mathbf{r}_1 \times \left\{\int_{\mathbf{r}_2} u_t(\mathbf{r}_2)\exp[-\omega(\mathbf{r}_{12})t]\mathrm{g}(\mathbf{r}_{12})d\mathbf{r}_2\right\}^{N-1} , \quad (2.3)$$

where $u_d(\mathbf{r}_1)$ and $u_t(\mathbf{r}_2)$ are, respectively, the spatial distributions of the donor and trap coil's sites, and $\mathrm{g}(\mathbf{r}_{12})$ is the site-to-site radial pair distribution function. The significance of $\mathrm{g}(\mathbf{r}_{12})$ in Eq. (2.3) is discussed below.

To perform the integrals in Eqs. (2.3), we adopt a multiframe coordinate system. The space containing the donor and trap distributions are spanned by the vectors $\mathbf{r}_1$ and $\mathbf{r}_2$, respectively. The donor–trap separations are then given by a coordinate transformation[21] that depends on the distance between the coil centers of gravity. Thus, $\mathbf{r}_2 = A\mathbf{r}'_{12}$, where $\mathbf{r}'_{12}$ spans the space containing the trap molecules in a newly defined coordinate system. The donor and trap distributions are modeled as Gaussian functions after the Gaussian chain model[37]

$$u_d(\mathbf{r}_1) = \left(\frac{3}{2\pi\langle R_\sigma^2\rangle}\right)\exp\left(\frac{-3}{2\langle R_\sigma^2\rangle}r_1^2\right) \quad (2.4a)$$

$$d\mathbf{r}_1 = r_1^2 \sin\theta_1\, dr_1\, d\theta_1\, d\phi_1 ,$$

$$u_t(\mathbf{r}_2) = \left(\frac{3}{2\pi\langle R_\sigma^2\rangle}\right)\exp\left(\frac{-3}{2\langle R_\sigma^2\rangle}r_2^2\right) \quad (2.4b)$$

$$d\mathbf{r}_2 = r_2^2 \sin\theta_2\, dr_2\, d\theta_2\, d\phi_2 .$$

Substitution of Eqs. (2.4) into Eq. (2.3) and further simplification by symmetry arguments results in

$$\langle G^s(t,R_s)\rangle = 2\pi\left(\frac{3}{2\pi\langle R_g^2\rangle}\right)^{3/2}\int_{r_1\theta_1}\int [G^s(r_1,\theta_1)]^{N-1} \times \exp\left(\frac{-3}{2\langle R_g^2\rangle}r_1^2\right) r_1^2 \sin\theta_1\, dr_1\, d\theta_1 , \quad (2.5a)$$

$$G^s(r_1,\theta_1) = 2\pi\left(\frac{3}{2\pi\langle R_g^2\rangle}\right)^{3/2} \times \int_{r_2\theta_2}\int \exp\{-\omega[r'_{12}(\theta_1,\theta_2,r_1,r_2)]t\} \times \mathrm{g}(r'_{12})\exp\left(\frac{-3}{2\langle R_g^2\rangle}r_2^2\right) r_2^2 \sin\theta_2\, dr_2\, d\theta_2 , \quad (2.5b)$$

where

$$|r'_{12}(\theta_1,\theta_2,r_1,r_2)|^2 = r_1^2 + r_2^2 + 2R_s[r_2\cos\theta_2 - r_1\cos\theta_1] - 2r_1r_2\cos(\theta_2-\theta_1) + R_s^2 \quad (2.5c)$$

and $\omega(r'_{12})$ is given by Eq. (2.2). Equations (2.5) express the excitation dynamics between two coils separated by the distance R_s. $\langle G^s(t,R_s)\rangle$ contains the details of the chromophore distributions and it represents the configurational average of the transport dynamics due to the pairwise interaction between two coils. This step reduces the calculation to the equivalent of transfer between two "effective chromophores." The internal structure of the chromophore clusters is contained in the calculation of $\langle G^s(t,R_s)\rangle$. This description of the coil transport dynamics, which contains only coil-to-coil transport interactions, is sufficient to model the copolymer concentration dependence of $\langle G^s(t)\rangle$.

B. DT calculations for tagged copolymers in the thermodynamic limit

An extension of Eqs. (2.5) to experimental observables must consider the effect of molecular interactions on both the intramolecular structure and the intermolecular site-to-site radial pair distribution function. A complete description of the bulk structure would include the complex interdependencies of the possible intra- and intermolecular conformations. This task has been addressed over the years by several workers.[2,3,9,10,38–43] The problem is vastly simplified by making use of the well-established fact that individual coils in dense melts and bulk glasses are ideal.[9,10] The concept of a θ condition as a reasonable description of the solid bulk state has been repeatedly verified in the literature.[43] In these situations, the forces which lead to intramolecular excluded volume are balanced by those forces arising from the interaction between molecules. The Flory postulate predicts that the segmental distribution of an ideal chain (θ condition) is Gaussian for distances beyond a few statistical segment lengths with a second moment that scales linearly with the chain size.[14] Since the chains in this study are *lightly* tagged with probe constituents (less than one probe per statistical seg-

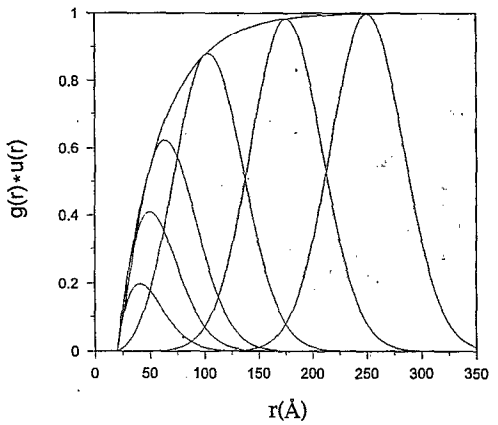

FIG. 1. A schematic representation of the effect of $g(r)$ on a Gaussian distribution of segments in one dimension. The acceptor chromophores (traps in DT transport) are assumed to have the same spatial distribution as the polymer segments. Gaussian functions with centers of mass close to the hard core are distorted. As the Gaussian center of mass is displaced to distances far from the reference position, the functional form of the Gaussian is restored.

ment length), the average interchromophore separation is large enough for the energy transport observable to reflect the Gaussian intramolecular chain structure.

The possibility of a perturbative affect of the chromophore tags on the intrachain structure was the subject of a previous study.[15] In that work, a tagged copolymer [poly(methylmethacrylate-co-2-vinylnaphthalene)] was prepared as a function of molecular weight and tagging fraction. It was shown that for lightly tagged chains, EET studies of the isolated tagged copolymers embedded in an untagged PMMA matrix resulted in measurements of the rms radius of gyration that are in perfect agreement with light scattering measurements made on the same molecular weight polymers in Θ condition solvents. Thus, the EET measurements are a nonintrusive probe of intramolecular chain structure in the bulk material. A similar analysis was performed on isolated tagged PMMA chains embedded in untagged poly(vinylacetate) (PVAc). In this case, the rms radius of gyration was found to be compressed relative to the values obtained from the corresponding measurements of the tagged polymers in bulk PMMA (~15% compression). This result too, was shown to be independent of the chromophore tagging fraction. Since the presence of chromophore substituents does not influence the intrachain structure, it is a reasonable inference that interchain structure is not affected either.

The pair distribution in Eq. (2.5) $g(r_{12})$ has the effect of modifying the trap coil's distribution of segments as seen by chromophore 1 on the donor coil. For example, if the trap coil is modeled as an ideal Gaussian distribution of chain segments, this Gaussian becomes distorted for donor–trap separations where the function $g(r_{12})$ deviates from unity. This approximation is illustrated for one dimension in Fig. 1. An exponential function with a 15 Å hard cutoff is arbitrarily shown to represent $g(r_{12})$. As the distance between the donor (chromophore 1) and the center of the trap distribution (chromophore 2) is decreased, the volume exclusion between sites 1 and 2 is reflected by a "perturbed" Gaussian function. In the limit of large distances, $g(r_{12})$ approaches unity and the intramolecular structure of the trap coil approaches the ideal Gaussian state.

The thermodynamic limit of $\langle G^s(t,R_s)\rangle$ can be achieved by averaging over the coil pair separation, R_s in the limit of infinite trap coil number and infinite volume. The ratio of trap coils to volume is restricted to equal the solution concentration. It is straightforward to obtain a copolymer concentration dependent expression for $\langle G^s(t,R_s)\rangle$ which includes an average intermolecular center-to-center radial pair distribution function $g_{\text{c.m.}}(R_s)$ (Ref. 21)

$$\langle G^s(t,\rho)\rangle = \exp\left\{-4\pi\rho\int_0^\infty [1-\langle G^s(t,R_s)\rangle] \times g_{\text{c.m.}}(R_s)R_s^2 dR_s\right\}, \tag{2.6}$$

where ρ is the copolymer solution concentration.

$g_{\text{c.m.}}(R_s)dR_s$ represents the probability that the center of mass of a polymer molecule lies within the radial distance R_s and R_s+dR_s from the reference coil's center of mass. For the purposes of this work, we assume that all intermolecular center-of-mass separations are equally probable such that $g_{\text{c.m.}}(R_s)=1$ for all R_s. This is a very good approximation for one-component systems. In binary blend systems, however, the center-to-center pair distribution will be an important characterization of the nature of nanodomain structure.

The form of the site-to-site $g(r_{12})$ serves to characterize the intermolecular structure as a measure of the degree of interpenetration among neighboring chain segments. The bulk may be comprised of ideal coils with segments that interpenetrate extensively. In this case, the intermolecular excluded volume only includes the "hard core" repulsions between chain segments. The site-to-site pair distribution function then has values remarkably close to unity for distances greater than the length characterizing the chain thickness. Alternatively, some melt or bulk systems may exhibit density fluctuations that occur on longer length scales which extend out to the radius of gyration. Recent x-ray scattering investigations of polyethylene melts[3] in combination with a tractable theoretical model have measured radial pair distribution functions dominated by hard core segmental repulsion. The form of $g(r_{12})$, in this case, was zero for distances less than 3.9 Å (associated with the cross sectional contact distance in polyethylene) followed by an extremely rapid approach to unity. Since theoretical predictions for more complicated systems are difficult, the EET experiments proposed in this work combined with Eq. (2.6) may provide a useful means to probe the form of $g(r_{12})$.

Equation (2.6) describes the decay of excitation probability in a concentrated tagged copolymer solution due solely to intercoil DT transfer events. Within the context of the adopted model, this is an exact solution to the DT problem for a system of interacting polymer molecules.

C. DD EET among tagged Gaussian chains in an untagged polymer host

The cumulant approximation for DD EET among chromophores distributed within interacting Gaussian surfaces was introduced by Marcus *et al.*[1,21] For the DD calculations, the donor and trap coils are chemically identical with each coil containing $N-1$ chromophores. It is consistent with the cumulant approximation to factor the Green's function into two independent contributions—an intra- and an interchain part

$$\langle G^s(t,\rho)\rangle = \langle G^s_{\rm on}(t)\rangle \langle G^s_{\rm off}(t,\rho)\rangle. \tag{2.7}$$

In Eq. (2.7), $\langle G^s_{\rm on}(t)\rangle$ describes transport "on" the coil containing the originally excited chromophore. This part of the energy transport is internal to the coil and can be calculated or measured independently from the interchain transport.[1] $\langle G^s_{\rm off}(t,\rho)\rangle$ describes forward and back transfer from the originally excited coil to chromophores on neighboring coils. This part of $\langle G^s(t,\rho)\rangle$ represents the interaction between coil pairs and is calculated as a configurational integral over pairwise interactions in direct analogy to the DT formulation presented above. The most notable differences between the DD and DT formulations are the following: Eqs. (2.5a) and (2.5b) are, respectively, replaced with

$$\langle G^s_{\rm off}(t,R_s)\rangle = 2\pi\left(\frac{3}{2\pi\langle R_g^2\rangle}\right)^{3/2}\int_{r_1\theta_1}\int G^s(r_1,\theta_1) \times \exp\left(\frac{-3}{2\langle R_g^2\rangle} r_1^2\right) r_1^2 \sin\theta_1\, dr_1\, d\theta_1 \tag{2.8a}$$

and

$$\ln G^s(r_1,\theta_1) = (N-1)\pi\left(\frac{3}{2\pi\langle R_g^2\rangle}\right)^{3/2} \times \int_{r_2\theta_2}\int \exp\{-2\omega[r'_{12}(\theta_1,\theta_2,r_1,r_2)]t\} \times g(r'_{12})\exp\left(\frac{-3}{2\langle R_g^2\rangle} r_2^2\right) r_2^2 \sin\theta_2\, dr_2\, d\theta_2. \tag{2.8b}$$

The definition of $r'_{12}(\theta_1,\theta_2,r_1,r_2)$ is defined as in Eqs. (2.5). The definition of $\omega(r)$ is the same as in Eq. (2.2) except that $R_0^{\rm DT}$ is replaced with $R_0^{\rm DD}$, the corresponding Förster critical distance for DD transfer. $\langle G^s_{\rm off}(t,\rho)\rangle$ is obtained from Eqs. (2.8) by the spatial average described by Eq. (2.6). This concentration dependent expression is then substituted into Eq. (2.7) to obtain the total Green's function decay $\langle G^s(t,\rho)\rangle$.

An important distinction between the DD and DT formulations is that there is no intracoil transfer present in the trap system. This allows the overall decay of G^s [Eq. (2.6)] to approach unity [instead of the intrachain function $\langle G^s_{\rm on}(t)\rangle$ as in Eq. (2.7)] as the coil concentration approaches zero.

D. DT calculations for the special case of tags on every chain

The EC formulations for $\langle G^s(t)\rangle$ depend on chromophore distributions which are not identical to the distribution of the polymer chain segments. This is due to the necessity of accounting for chromophore correlations between tags on the same chain by employing the Gaussian approximation for intramolecular chain structure. The transport observable for two chains, as expressed by Eq. (2.3), contains the site-to-site pair distribution through an average over the Gaussian structure of the acceptor chain (an integration over the space spanned by $\mathbf{r}_2$). This is followed by an average over the donor chain distribution (spanned by $\mathbf{r}_1$). In addition to these averages, the observable measured in an experiment contains the additional spatial average in the thermodynamic limit [Eq. (2.6)]. Hence, $\langle G^s(t)\rangle$ obtained from a fluorescence measurement of tagged guest chains in an untagged host is a complicated function of the site-to-site radial pair distribution.

If chromophores are randomly placed on every molecule, the distribution of tags is then a representation of the distribution of chain segments. In this case, the Gaussian approximation made in the EC method is not necessary and the transport observable is more closely related to the site-to-site pair correlation function. Fredrickson has given a derivation for DT EET among chromophores attached to the ends of polymer chains.[6] In that work, the fluorescence observable depends on the radial pair distribution function of chain ends. Here, a formulation for DT and DD transfer among chromophores randomly tagged to any part of the chain is given. For the DD case, the two particle cumulant approximation is employed.[32] Unlike the end tagged experiment proposed by Fredrickson, the experimentally determined decay of $\langle G^s(t)\rangle$ in a randomly tagged system depends directly on the site-to-site pair correlation function of chain segments. As in the EC formulation above, the donor chains each contain a single donor chromophore, while the acceptor chains may have one or more acceptor chromophores randomly distributed along their lengths. In the case of DT transport, the number of donor chains is small compared to the number of trap chains, so that statistically every donor is surrounded by traps. The position of the donor molecule is translationally invariant and the following equation can be derived from Eq. (2.3):[6]

$$\langle G^s_{\rm off}(t)\rangle = \left[\frac{4\pi}{V}\int_0^{R_v}\left(\frac{1}{2}\{1+\exp[-2\omega(r)t]\}\right) \times r^2 g(r)dr\right]^{N-1} \quad \text{(DD)} \tag{2.9a}$$

and

$$\langle G^s_{\rm off}(t)\rangle = \left(\frac{4\pi}{V}\int_0^{R_v}\exp[-\omega(r)t] \times r^2 g(r)dr\right)^{N-1} \quad \text{(DT)} \tag{2.9b}$$

where the distribution of acceptors has been chosen as $u_t(r)=(4\pi r^2)/V$, $V=(4\pi R_v^3)/3$, $R_v=[(3N)/(4\pi\rho)]^{1/3}$, $\rho=N/V$, and $\omega(\mathbf{r})$ is given by Eq. (2.2). Note that ρ has the meaning of trap chromophore concentration. Equations (2.9) are taken in the limit of infinite acceptor number and volume such that the concentration ρ is held constant. Thus, in the thermodynamic limit, Eqs. (2.9) become

$$\langle G^s_{\text{off}}(t)\rangle=\exp\left(-\frac{4\pi\rho}{\lambda}\int_0^\infty\{1-\exp[-\lambda\omega(r)t]\}r^2\mathrm{g}(r)dr\right), \tag{2.10}$$

where $\lambda=1$ for DT transport and $\lambda=2$ for DD transport. As in the EC formulation, $\langle G^s_{\text{off}}(t)\rangle$ represents interchain transfer events and its relation to the total decay of the Green's function is given by Eq. (2.7). For the DT case, there is no intrachain transfer and $\langle G^s(t)\rangle = \langle G^s_{\text{off}}(t)\rangle$. For the case of DD transfer, however, the intrachain transfer processes make a contribution to the overall decay of initial excitation probability.

It has been shown by Ohmine *et al.*[44] that $\mathrm{g}(r)$ can be extracted from fluorescence measurements which obey the form of Eq. (2.10) by a Laplace transformation

$$\langle G^s(t)\rangle=A\ \exp\left[\rho\int_0^\infty \mathrm{g}(s)\exp(-st)ds\right], \tag{2.11}$$

where $A=e^{-N}$, $s=\lambda\omega(r)$, and $\mathrm{g}(s)=(1/\lambda)[(2\pi\tau_F)/(3R_0^6)]r^9\ \mathrm{g}(r)$. This implies that for systems with tags on every chain, there is a one to one correspondence between the function $\langle G^s(t)\rangle$ and the site-to-site pair correlation function.

It is useful to compare Eq. (2.10) to the solution for the case $\mathrm{g}(r)=1$ for all r. This is the well-known Förster result for direct trapping in random, isotropic DT systems and the cumulant result for random, isotropic DD systems[32]

$$\langle G^s_{\text{off}}(t)\rangle=\exp\left[-\frac{4}{3}\pi R_0^3\lambda^{-1/2}\rho\Gamma\left(\frac{1}{2}\right)\left(\frac{t}{\tau_F}\right)^{1/2}\right], \tag{2.12}$$

where $\Gamma(\frac{1}{2})=1.7725$. In the polymer system, the extent to which $\langle G^s(t)\rangle$ deviates from Eq. (2.12) is a measure of the depth and shape of the correlation hole.

Until recently, the conventional methods used to study the correlation hole effect in polymer melts and in the bulk have involved x-ray or neutron scattering measurements.[45] In general, the experimental observable measured in a scattering experiment is the structure factor $\hat{S}(k)=\hat{S}_{\text{intra}}(k)+\rho\hat{h}(k)$.[46] The relationship between the scattering observable and the pair correlation function is given by a Fourier transformation

$$\hat{h}(k)=\int \exp[-i\mathbf{k}\cdot\mathbf{r}]h(r)d\mathbf{r}, \tag{2.13}$$

where $\hat{S}_{\text{intra}}(k)$ is the single chain structure factor, $h(r)=\mathrm{g}(r)-1$ is called the total correlation function and $k=(4\pi/\lambda)\sin(\theta/2)$ is the magnitude of the scattering wave vector. Again, there is a one to one correspondence between the scattering observable and the pair correlation function. A comparison between Eqs. (2.11) and (2.13) suggests an apparent analogy between the fluorescence and scattering experiments. In principle, all of the information contained in the functional form of $\mathrm{g}(r)$ is transformed into the time or wave vector domains through the transformations given by Eqs. (2.11) and (2.13), respectively. The corresponding inverse transformations can be used to recover $\mathrm{g}(r)$ from these measurements. In practice, however, this is difficult because noise in the data can lead to gross inaccuracies in $\mathrm{g}(r)$. Thus, the most important limitation to high resolution measurements of $\mathrm{g}(r)$ is determined by the experimental signal to noise ratio. Until recently, the signal to noise ratio associated with conventional time resolved fluorescence techniques has prevented the direct inversion of the observable to obtain $\mathrm{g}(r)$. The development of state of the art detection techniques, such as time correlated single photon counting, has made it possible to obtain data that is essentially free of noise. Therefore, it is now possible to obtain a model independent measurement of $\mathrm{g}(r)$ by direct inversion of the time resolved fluorescence observable.

III. THE RELATIONSHIP BETWEEN $\langle G^s(t)\rangle$ AND THE SITE-TO-SITE PAIR CORRELATION FUNCTION

In the previous section, it was shown that $\langle G^s(t)\rangle$ may be a complicated function of the pair correlation function. As suggested by other workers,[6,44] the most straightforward method of extracting structural information from experimental data is to make a comparison with Eq. (2.6) after a proposed form for $\mathrm{g}(r)$ has been inserted into Eqs. (2.5). Since we are interested in examining the sensitivity of the calculations to the functional form of $\mathrm{g}(r)$, we employ model test functions for this purpose.

A. Model radial pair distribution functions for the site-to-site $\mathrm{g}(r)$

Recent investigations by Narten *et al.*[47] and Honnell *et al.*[3] of polyethylene melts suggest the dominant feature of $\mathrm{g}(r)$ in this system is the monomeric hard core exclusion which depends on the contact distance associated with the site-to-site interaction. However, under certain conditions, the correlation hole may occur on the distance scale of the radius of gyration. For simplicity, we choose to model these situations with the following distributions:

$$\mathrm{g}(r)=H(r-\sigma)=0, \quad \text{if } r\leqslant\sigma=1, \quad \text{if } r>\sigma, \tag{3.1}$$

$$\mathrm{g}(r)=1-\exp[-(r-\sigma)/\lambda]. \tag{3.2}$$

The Heaviside step function (3.1) contains a hard core excluded volume effect which turns on at the contact diameter σ. A "softer" excluded volume that abruptly turns on at σ and then continues to climb toward unity can be simulated using Eq. (3.2). The "depth" of the hole depends on the characteristic length λ. A small value for λ corresponds to a deep hole, since this means $\mathrm{g}(r)$ is primarily the hard core interaction, and interpenetration among chain segments is otherwise complete. Progressively larger values of λ result in more shallow holes corresponding to the exclusion of segments belonging to other chains. In this context, Eq. (3.2) is strictly a phenomenological function that will serve to qualitatively model long range correlations.

A more physically significant form for the intermolecular pair correlation function can be obtained from the Gaussian string approximation to the reference interaction site model (RISM) theory for homopolymer melts.[48] The string model is based on linear chains of hard spheres characterized by intersphere separations given by the statistical segment length l and the sphere diameter σ. Implicit in the model is a large separation between local and global length scales such that the dimension of the chain (R_g) is large in comparison to σ and l. The "aspect ratio" $\Gamma=l/\sigma$ is a measure of the chain stiffness with $\Gamma>1$ corresponding to a stiff chain and $\Gamma<1$ corresponding to a flexible chain. For the Gaussian string, the analytical approximation to RISM for $g(r)$ has a screened Coulomb or Yukawa form.

$$g(r)=1-\frac{3}{\rho_m l^3 \pi r}[\exp(-r/\xi_c)-\exp(-r/\xi_p)], \quad (3.3)$$

where ρ_m is the site density of the monomers and is related to the packing density $\eta=[(\pi\rho_m\sigma^3)/6]$. The two correlation lengths in Eq. (3.3) represent different properties of the chains in the melt. ξ_c is called the "correlation hole" length scale associated with the size of the chain and is given by $R_g/\sqrt{2}$. ξ_p is a density dependent short range correlation due to collective density fluctuations. It depends on the segmental density, the aspect ratio, and the radius of gyration through the transcendental equation

$$\xi_p(\xi_p+\Gamma^{-1})\exp[-(\Gamma\xi_p)^{-1}]-\xi_p^2 = \frac{\pi}{9}\rho_m\sigma^3+\frac{R_g}{\sqrt{2}}\left(\frac{R_g}{\sqrt{2}}+\Gamma^{-1}\right)\exp(-\sqrt{2}\Gamma^{-1}R_g^{-1})-\frac{R_g^2}{2}. \quad (3.4)$$

Equations (3.3) and (3.4) for the Gaussian string model have been shown to agree quite well with numerical RISM calculations on Gaussian chains having finite size hard core diameters.[47]

In Figs. 2(a) and 2(b), plots of Eqs. (3.2) and (3.3) are shown as functions of λ, ξ_c, and ξ_p, respectively. Because experiments discussed below employ naphthalene as the chromophore, the hard core interaction distance was chosen to be consistent with the hard sphere naphthalene diameter obtained from crystalline naphthalene ($\sigma\sim6$ Å). In Fig. 2(a), the distribution function (3.2) that approaches unity most rapidly has $\lambda=0.01$ Å. This is essentially the Heaviside step function with $\sigma=6$ Å. Subsequently, longer range correlations have $\lambda=1$, 5, 10, and 15 Å. In Fig. 2(b) Eq. (3.3) has been plotted for five different values of the aspect ratio Γ. For this calculation, the parameters characterizing the polymer system were chosen to be similar to the experimental system (naphthyl-tagged PMMA in untagged PMMA) investigated in Ref. 1. The radius of gyration was fixed at $R_g=57.9$ Å, the hard core distance was fixed at 6.0 Å, and the packing fraction was fixed at a value of $\eta=0.5$ typical of liquids. The statistical segment length (and consequently, the number of statistical segments) were varied to change the aspect ratio. The curves shown in Fig. 2(b) are based on $\Gamma=0.83$, 0.91, 1.0, 1.1, and 1.2. The corresponding values for ξ_p obtained from Eq. (3.4) and used in Eq. (3.3) are $\xi_p=4.6$, 3.5, 2.5, 1.6, and 0.032 Å, respectively. The value used for ξ_c was 41 Å. Increasing the aspect ratio has the effect of stiffening the chain, resulting in less intramolecular screening and causing the correlation hole to become shallower.

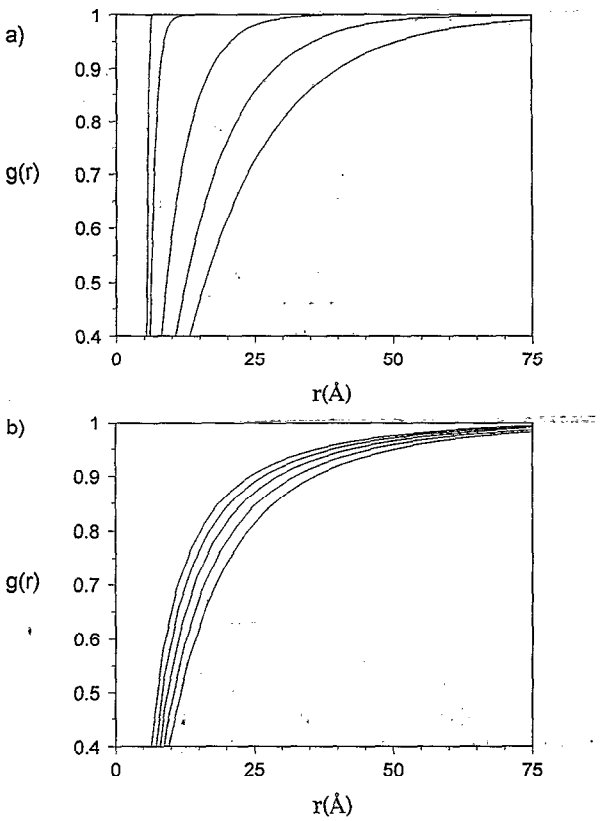

FIG. 2. A comparison of model intermolecular segmental pair distribution functions. (a) The model distribution is an exponential function given by Eq. (3.2) with $\sigma=6$ Å. The values of λ are 0.1, 1, 5, 10, and 15 Å. (b) The distribution is a Yukawa function given by Eq. (3.3) with $\sigma=6$ Å. The value of $\xi_c=41$ Å. The values of ξ_p are (in order of shallower holes) 4.6, 3.5, 2.5, 1.6, and 0.032 Å, respectively.

IV. RESULTS AND DISCUSSION

The application of fluorescence EET measurements toward the elucidation of intermolecular structure in melts, the bulk, or polymer solutions depend on the resolving power of the technique. The function $\langle G^s(t)\rangle$ is obtained from time dependent fluorescence measurements which may be performed for a variety of time scales (10^{-14}–10^{-7} s). A typical method employs time correlated single photon counting.[49] This approach has several advantages-a low excitation pulse power ($\sim nJ$), good time resolution ($\sim$50 ps), and excellent signal to noise. Since the method involves the accumulation of data over many excitation shot cycles, the signal to noise improves as a function of acquisition time. In most cases, data may be collected over a long enough period to optimize the signal to noise ratio. Thus, it is possible to obtain extremely accurate data which are relatively free of noise.

TABLE I. Physical characteristics of the guest [poly(co-2-vinylnapthylene-methylmethacrylate)] and host [poly(methylmethacrylate)] polymers. M_w is the weight average molecular weight, M_w/M_n is the polydispersity, %2-VN is the number percent naphthyl subunits, $\langle N_{chrom}/coil\rangle$ is the average number of chromophores per molecule, N_{mon} is the number of monomers per molecule, N_{stat} is the number of statistical segments per molecule, and $\langle R_g^2\rangle^{1/2}$ is the rms radius of gyration based on the random coil model.

Polymer	M_w	M_w/M_n	%2-VN	$\langle N_{chrom}/coil\rangle$	N_{mon}	N_{stat}	$\langle R_g^2\rangle^{1/2}$
Guest	51 900	1.47	6.5	32	501	80.2	57.9 Å
Host	93 300	2.01	0	0	932	149	79.1 Å

A. Experimental DD investigation—naphthyl tagged PMMA guest in an untagged PMMA host

Previously, experiments were carried out on solid mixtures of 6% tagged poly(methyl methacrylate-co-2-vinylnaphthalene) in a poly(methyl methacrylate) host.[1] In this study, time resolved fluorescence depolarization measurements of the naphthyl probes were made as a function of copolymer concentration. The physical characteristics of the system are reported in Table I. Six different samples, each with a different concentration, were examined.

In addition to the volume fraction of the guest polymer, it is useful to consider the reduced concentration defined by[45]

$$c^* = \frac{\rho N_A}{M_w}\frac{3}{4}\pi R_g^3. \tag{4.1}$$

This is approximately the average number of guest polymer chains which can be found in a spherical volume of radius R_g. For reduced concentrations larger than one, there is significant overlap between the tagged polymers, while for more dilute concentrations, there is little or no overlap. These and other relevant parameters characterizing the samples are reported in Table II.

Figure 3 shows a comparison between fluorescence anisotropy data originally presented in Ref. 1 and theoretical calculations based on the EC method for DD transport.[50] The data are constructed from the time dependent parallel and perpendicular intensities by point by point addition according to Eq. (1.2). The calculations are obtained by numerical integration of Eqs. (2.8) and (2.6) for a particular concentration. The resulting function $\langle G^s_{off}(t,\rho)\rangle$ is related to the anisotropy through

TABLE II. Intercoil EET samples. Vol. % is the copolymer volume percent, τ is the measured radiative fluorescence lifetime, width is the sample thickness, c^* is the calculated reduced copolymer concentration [from Eq. (6.20)], $\langle R_{sepr}\rangle$ is the mean separation between copolymer centers of mass, and O.D. is the measured optical density at the absorption maximum (λ_{max}=320 nm).

Vol. %	τ (ns)	Width (μm)	c^*	$\langle R_{sepr}\rangle$ (Å)	O.D.
20.0	47.2	40	2.3	27	0.2
10.0	48.6	80	1.1	35	0.2
5.0	50.0	150	0.6	43	0.19
2.5	50.5	300	0.3	54	0.19
3/8	49.0	1600	0.04	105	0.15
1/8	49.0	1600	0.01	167	0.05

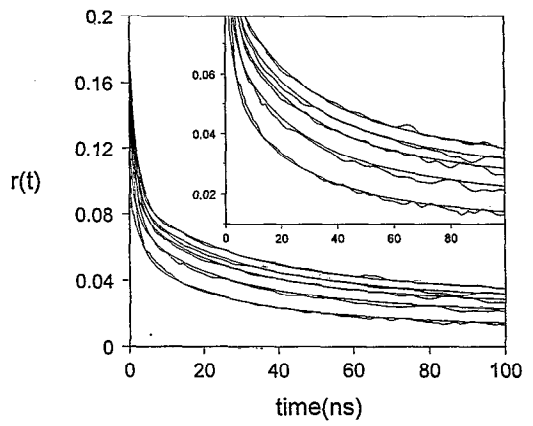

FIG. 3. Time-dependent anisotropy decays and theoretical calculations for the P(2VN-MMA)/PMMA DD systems characterized by Tables I and II. For these calculations, R_0=12.3 Å and the segmental radial pair distribution function $g(r)=1$ for all r. The lowest copolymer concentration (vol. %=0.125%) decays the least and represents intramolecular energy transfer. Subsequently decreasing decays contain contributions from intermolecular energy transfer for copolymer concentrations 2.5%, 5%, 10%, and 20%.

$$r(t,\rho) = r_{on}(t)\langle G^s_{off}(t,\rho)\rangle. \tag{4.2}$$

Here, $r_{on}(t)$ represents the experimentally determined fluorescence anisotropy due to depolarization processes that occur on isolated, noninteracting polymer coils. It contains the intracoil EET as well as contributions to the anisotropy from chromophore rotation. Since we are only interested in intercoil EET, for simplicity the measured anisotropy of the isolated coil was fit to a triexponential function

$$\begin{aligned} r_{on}(t) = {} & 0.0968\ \exp[-(t/1.67\ \text{ns})] \\ & + 0.0469\ \exp[-(t/25.7\ \text{ns})] \\ & + 0.043\ \exp[-(t/457\ \text{ns})]. \end{aligned} \tag{4.3}$$

Equation (4.3) provides a smooth curve for use in Eq. (4.2). The isolated coil data were obtained from the most dilute samples (ρ=0.375% and 0.125%) listed in Table II. The anisotropies obtained from both of these low-concentration samples were identical, indicating that the dilute, intracoil EET limit had been achieved.

The fluorescence lifetimes of all the samples were determined from the total fluorescence $I_{tot}(t)=I_{\parallel}(t)+2I_{\perp}(t)$. These decays were monoexponential with radiative lifetimes listed in Table II. The independence of τ on concentration and the monoexponential form of $I_{tot}(t)$ indicate the absence of concentration dependent processes such as excimer trapping or radiative reabsorption.

For the calculations presented in Fig. 3, the intermolecular site-to-site pair distribution function $g(r)=1$ for all r, corresponding to the absence of a correlation hole. The orientationally dependent Förster transfer distance R_0 = 12.3±0.6 Å.[16] The intracoil decay (ρ=0.375%) is the slowest. The calculated line through these data is Eq. (4.3). The curves that lie below represent intercoil EET for concentrations ρ=2.5%, 5%, 10%, and 20%. As the coil concentration is increased, the rate of EET also increases. This shows

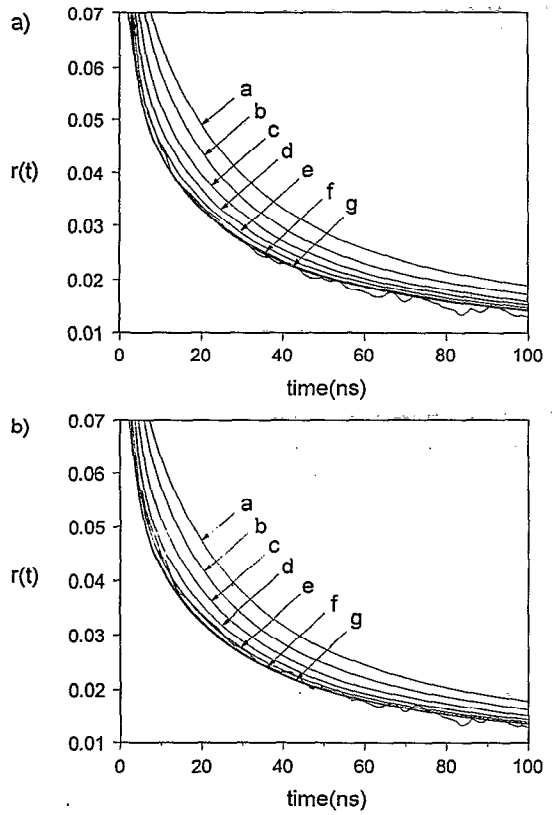

FIG. 4. Comparisons of experimental time-dependent anisotropy decay for the 20% sample with theoretical calculations based on hard shell $g(r)$ given by Eq. (3.1). In (a) $R_0=12.3$ Å, while in (b), $R_0=12.8$ Å. In both figures, the decays correspond to $\sigma=(a)$ 12; (b) 10; (c) 8; (d) 6; (e) 4; (f) 2; and (g) 0 Å.

that at these copolymer concentrations, intercoil EET is effectively competing with intracoil EET. The slight disagreement for the highest concentrations at very short time is due to a trace fluorescent impurity in the host PMMA. The fluorescence from this impurity occurs only at very short time and is detectable for the lowest concentration samples (3/8% and 1/8%). This leads to a small inaccuracy of Eq. (4.3) at very short time which is amplified by Eq. (4.2). Despite this difficulty, the theoretical calculations with no adjustable parameters are in quantitative agreement with the data. The theory, based on a random distribution of ideal polymer coils, correctly predicts both the amplitude and the functional form of the anisotropy decays.

Although Eq. (4.2) fits the data exceptionally well, it is necessary to analyze the sensitivity of these calculations to the possible form of $g(r)$. Clearly, the assumption $g(r)=1$ for all r is unrealistic for distances smaller than the hard core contact distance associated with the naphthyl substituents. Figures 4(a) and 4(b) show a comparison of the 20% data with calculated anisotropies based on the hard shell cutoffs given by Eq. (3.1). In Fig. 4(a), the Förster distance $R_0=12.3$ Å, while in Fig. 4(b), it has been set equal to 12.8 Å, which is within the error bar associated with R_0. In both figures, the values of σ are 0, 2, 5, 6, 8, 10, and 12 Å. The fastest calculated decays correspond to the smallest contact distances. Increasing the magnitude of σ tends to slow the theoretical decays because the coil segments are prevented from interpenetrating to this extent. In Fig. 4(a) (which uses the smaller of the two values for R_0), the calculations for $\sigma=0$ and 2 Å are almost indistinguishable and appear to fit the data best at times longer than 10 ns, although at shorter times, the calculation with $\sigma=5$ Å follows the data more closely. For $\sigma=6$, 8, 10, and 12 Å, the agreement is poor, indicating a range of contact values that are clearly inconsistent. In Fig. 4(b), the calculations for $\sigma=0$ and 2 Å fall below the data, most noticeably during the first 50 ns. The calculation for $\sigma=5$ Å, however, is consistent with the data. Subsequently larger values for σ decay much slower than the data. The functional form of the theoretical decays appear to match the data more closely when the larger value for R_0 (12.8 Å) is used.

In the previous experimental study, the physical significance of the contact parameter σ was interpreted as a measure of the cross sectional dimension of the polymer chain. To estimate the chain cross section, we constructed a molecular model consisting of three methylmethacrylate subunits. According to this model, an approximate value of $\sigma=10$ Å was determined. In light of the results presented in Figs. 4(a) and 4(b), however, this value appears too large to be in agreement with the data. It is possible that a more accurate interpretation of $g(r)$ in this experiment would involve a sidechain site-to-site pair distribution function. In this case, it is reasonable to associate the value of σ with the dimension of the naphthyl chromophore substituent (~6 Å). The comparisons made in Figs. 4(a) and 4(b) serve to illustrated the sensitivity of the DD calculations to the hard core cutoff. Further studies could improve the determination of R_0, making statements about the value of σ even more quantitative.

Figure 5 shows comparisons of experimental data and the DD calculations for $\rho=20\%$ based on the model radial distributions given by Eqs. (3.2). The value of R_0 used in these calculations is 12.3 Å. In Fig. 5(a) the fastest decay corresponds to the radial distribution given by Eq. (3.1) with $\sigma=6$ Å. Subsequently slower decays correspond to Eq. (3.2) with increasing values of $\lambda=1$, 5, 10, and 15 Å. The smallest

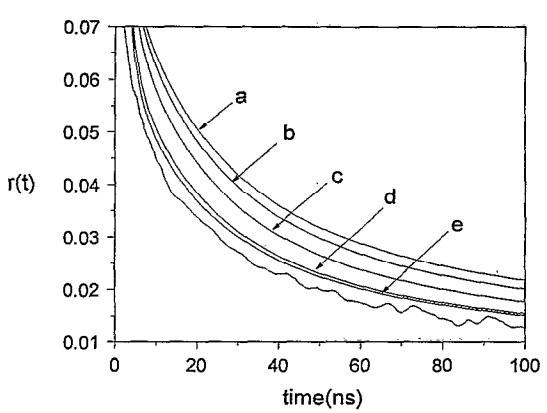

FIG. 5. Comparisons of theoretical time-dependent anisotropy decays and experimental data for the 20% sample based on the model distribution described by Eq. (3.2). The decays correspond to the exponential function (3.2) with $\sigma=6$ Å and $\lambda=$(a) 15; (b) 10; (c) 5; (d) 1; and (e) 0.1 Å.

length $\lambda=1$ Å is only slightly distinguishable from the hard shell distribution. Larger values of λ, however, are obviously very different from the hard shell, and can be easily distinguished from data. These comparisons strongly suggest that the form of $g(r)$ in this system resembles the most narrow hole distributions shown in Fig. 2(a). Similar to the findings of Honnell *et al.*, the correlation hole must consist primarily of a hard core contact interaction between the chromophore substituents, in this case, ≤ 6 Å.

B. DT calculations for tagged Gaussian chains in an untagged host

For the DD calculations presented above, the limitations in the sensitivity of $r(t)$ to $g(r)$ can be understood in terms of the relative contribution to the fluorescence anisotropy from both intra- and interchain energy transfers. According to Eq. (4.2), the anisotropy of the system of interacting tagged polymers contains a multiplicative factor $r_{on}(t)$ due to the intrachain EET. Since $r_{on}(t)$ may be small for all t, a detectable change in $r(t)$ may require a relatively significant change in the factor $\langle G^s_{\text{off}}(t,\rho)\rangle$ describing the concentration dependent interchain transport. Therefore, a detailed examination of the interchain structure is limited by intrachain transfer processes that compete with the interchain processes we are interested in. This problem, however, is eliminated when considering the equivalent DT situation.

Figures 6–9 show plots of DT calculations for two types of systems described above. In one case, only some of the trap chains have chromophore tags, and in the other case, all chains (except the donor chain) are tagged. In both cases, the experimental observable is the time dependence of the total fluorescence intensity which is related to $\langle G^s(t)\rangle$ through Eq. (1.4). For all the DT calculations presented below, the value used for $R_0^{\text{DT}}=12.3$ Å and that used for the fluorescence lifetime $\tau_F=50$ ns.

Figures 6(a) and 6(b) show comparisons of calculated decays of $\langle G^s(t)\rangle$ and the normalized total donor fluorescence $I(t)/I_0$ using the hard core cutoffs given by Eq. (3.1). In these calculations, $\rho=5\%$. The values of σ are the same as those used in Figs. 4(a) and 4(b). The DT calculations display similar behavior to the DD calculations discussed above. The most important difference is that the resolution appears to be much better for the DT case, due to the absence of intrachain transport processes.

If tags are placed on every polymer molecule as described in Sec. II D, the decay of $\langle G^s(t)\rangle$ is described by Eq. (3.5). Figures 7(a) and 7(b) show hard core calculations for $\langle G^s(t)\rangle$ and $I(t)/I_0$, respectively. In these calculations, the concentration of naphthyl substituents is chosen such that $\rho=10^{20}$ cm^{-3}. For a system of tagged molecules with $M_w=51\,900$ and the density of PMMA (1.2 g cm^{-3}), this corresponds to seven traps per chain with a small number of chains having a single donor. The values of σ are the same as those used in Figs. 4 and 6. A comparison between Figs. 6 and 7 shows that the effect of tagging every chain results in a different functional form in the decay of $\langle G^s(t)\rangle$ then when only some of the chains are tagged (EC method). The EC calculations characteristically have a rapidly decaying component at short time (<20 ns) followed by a slower component at longer times. In contrast, the system with tags on every chain demonstrates a more uniform decay of $\langle G^s(t)\rangle$ over two fluorescence lifetimes. Another important distinction is the difference in sensitivity. While the hard core decays with $\sigma=0$ and 2 Å are distinguishable from one another for the EC calculations, they are not when every chain has tags. For hard core interactions alone, the EC method appears to be more sensitive to the size of σ than Eq. (2.10).

A comparison between the sensitivity of the EC method and the 100% tagged chain system to the pair correlation function given by Eq. (3.2) is given in Figs. 8(a) and 8(b), respectively. The values used for σ and λ are the same as those used in Fig. 5. Again, the pattern established in the DD calculations is repeated. Similar to the hard core comparisons above, the EC method is slightly more sensitive to the form of the long range correlations determined by λ.

It is clear from the above comparisons that the DT EC method is more sensitive to the form of $g(r)$ than the 100% tagged DT method which in turn is more sensitive than the DD EC method. DD calculations for tags on every chain will show comparable sensitivity to $g(r)$ as the DT 100% tagged system, although it will be slightly worse due to the intrachain contribution to the total decay. This intrachain part, however, will be relatively unimportant since there are only a few chromophores per polymer chain (~7).

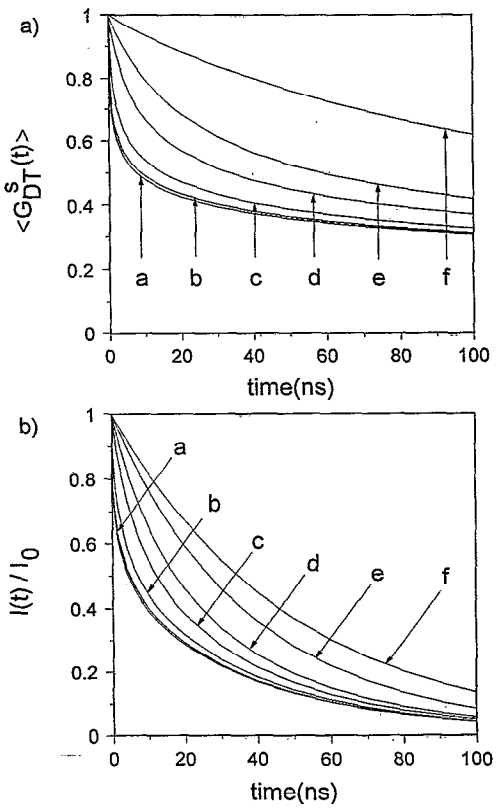

FIG. 6. Comparisons of DT calculations for the 5% tagged polymer system described in Table I. The calculations are based on the hard core model distribution functions given by Eq. (3.1). In (a) the decays of $\langle G^s(t)\rangle$ are shown. Values of σ are (a) 0; (b) 2; (c) 4; (d) 6; (e) 8; (f) 10 Å. In (b) the decay of the normalized total fluorescence is shown (based on $\tau_F=50$ ns). The values of σ are (a) 0 and 2; (b) 4; (c) 6; (d) 8; (e) 10; and (f) 12 Å.

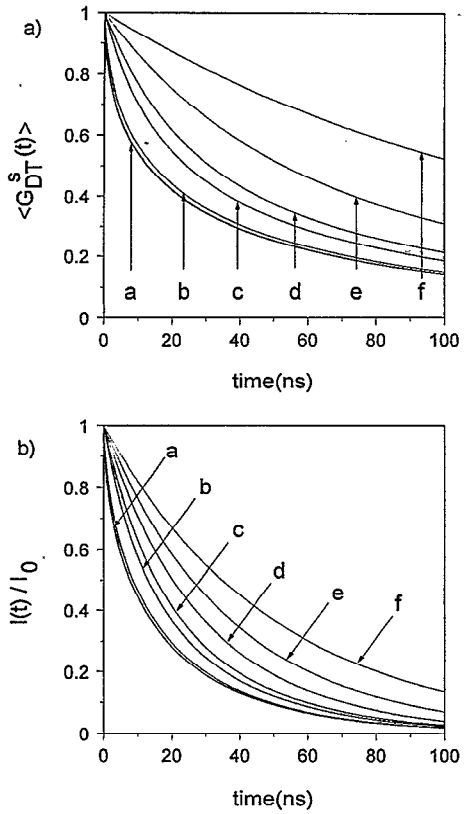

FIG. 7. Comparisons of DT calculations for a 100% tagged polymer system described in Sec. IV C. The calculations are based on the hard core model distribution functions given by Eq. (3.1). In (a), the decays of $\langle G^s(t)\rangle$ are shown. Values of σ are (a) 0 and 2; (b) 4; (c) 6; (d) 8; (e) 10; (f) 12 Å. In (b), the decays of the normalized total fluorescence is shown (based on $\tau_F=50$ ns). The values of σ are labeled as in Fig. 8(a).

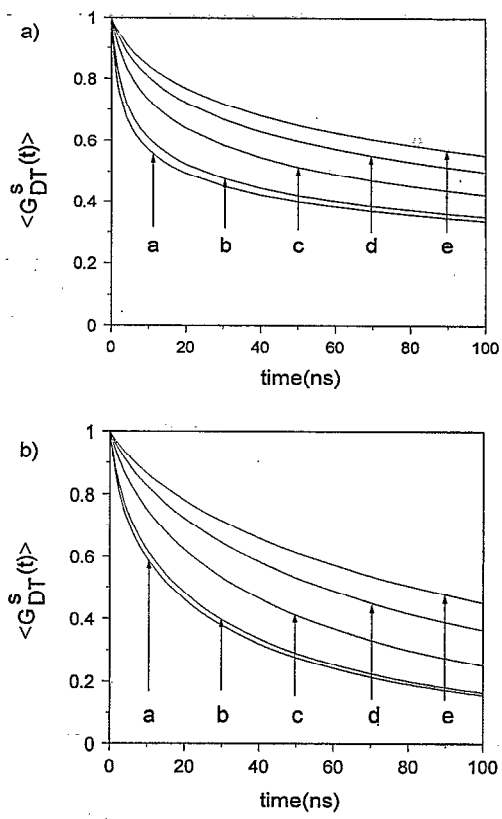

FIG. 8. Comparisons of DT calculations for (a) the 5% tagged polymer system (EC method) and (b) the 100% tagged DT system. The calculations are based on the exponential model distribution described by Eq. (3.2). In both figures, the decays correspond to the values $\sigma=6$ Å and $\lambda=$(a) 0.1; (b) 1; (c) 5; (d) 10; (e) 15 Å.

DT calculations for the 100% tagged system based on pair correlation functions obtained from the Gaussian string model [Fig. 2(b)] are shown in Fig. 9. Since the sensitivity of this system is comparable to the EC approach, Fig. 9 serves to illustrate the effect of changing the chain's aspect ratio. The values used for the aspect ratio are the same as those used in Fig. 2(b). The effect of stiffening the chain leads to a more shallow correlation hole and a subsequently slower decay of $\langle G^s(t)\rangle$. These differences can be distinguished in an experiment.

V. CONCLUDING REMARKS

The analysis presented above is the first detailed examination of the dependence of excitation transport on the intermolecular pair distribution function $g(r)$ in a controlled system of concentrated tagged polymer coils. The results indicate that calculations of fluorescence observables, based on the configurational models depicted here, are extremely sensitive to the form of $g(r)$.

Comparisons between theoretical predictions and experimental data taken from Ref. 1 suggest that the form of $g(r)$ consists primarily of a hard core contact interaction between the naphthyl chromophore substituents (~6 Å). For this system, atactic 6% poly(methyl methacrylate-co-2-vinylnaphthalene) in atactic poly(methyl methacrylate), the chromophore probes are intrinsic side group components of the polymer molecules. Therefore, a more accurate interpretation of $g(r)$ will involve a model that describes the side group pair distribution function. More detailed information can be obtained from this data provided the value of the Förster

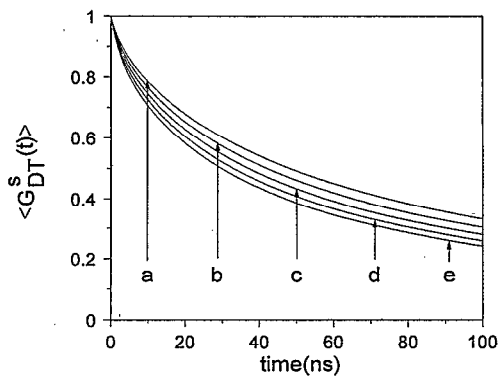

FIG. 9. DT calculations for a 100% tagged polymer system described in Sec. II D. The calculations are based on the pair correlation functions described by Eq. (3.3). The values used for σ, ξ_c, and ξ_p are the same as those used in Fig. 2(b). The differences in the decays illustrate the sensitivity of the method to an intramolecular property such as chain stiffness.

transfer distance is determined to a higher degree of precision.

An important consequence of the above comparison between theory and data is that current models for chain–molecule fluids are not sufficient to describe real systems. Most theories involve simplified models such as the freely jointed "pearl necklace" hard chain, in which molecules are composed of tangentially bonded hard spheres.[51] Typically, the sphere diameter determines the nearest neighbor contact distance, since this is the closest approach between two segments. In some approaches, the sphere diameter is equal to the statistical segment length. For the experimental PMMA system, $l_{stat} \cong 16$ Å. This is clearly inconsistent with the nearest neighbor distance (~5–6 Å) determined in the analysis. A more realistic model will involve internal structure which can account for the locations of the chromophore substituents. Such calculations are possible using multisite polymer RISM theory, where the intramolecular structure is accounted for in a realistic manner.

Analogous DT calculations exhibit an improvement in sensitivity relative to the DD results. This is due to the absence of an intrachain contribution to the transport observable, which is present in the DD system.

The above DT analysis makes use of the EC method for clustered chromophore systems. A comparison between the EC method and DT calculations for a polymer system with tags on every chain demonstrates that the EC method is slightly more sensitive to the form of $g(r)$. There are advantages, however, to experiments on systems with every chain tagged. In contrast to the multidimensional numerical integration involved in the EC approach, the fluorescence observable is simply expressed as a one-dimensional integral [Eq. (3.5)]. In addition, the preparation of samples do not require careful measurements of tagged copolymer concentrations. It is possible that systems with tags on every chain may be the best choice for studies of intermolecular chain structure in single component systems.

The EC method will be necessary for the investigation of intermolecular chain structure in binary component systems. The structure and dynamics associated with nanophase separated domains in these mixtures requires a model which involves transport among interacting clusters of chromophores. Similar work can be used to obtain correlation hole information in block copolymer systems. An accurate description of EET in the presence of dynamical disorder may be applied to related problems such as structure elucidation and dynamics in biomolecular systems.

ACKNOWLEDGMENTS

We would like to thank Professor Kenneth S. Schweizer for helpful discussions. This work was supported by Department of Energy, Office of Basic Energy Sciences (contract DE-FG03-84ER13251). We would also like to thank the Stanford Center for Materials Research Polymer Thrust Program for additional support and acknowledge an NSF departmental instrumentation grant (No. CHE 88-21737) which provided computer equipment used in the calculations.

[1] A. H. Marcus, N. A. Diachun, and M. D. Fayer, Macromolecules **26**, 3041 (1993).
[2] K. S. Schweizer and J. G. Curro, J. Chem. Phys. **96**, 3211 (1992).
[3] K. G. Honnell, J. D. McCoy, J. G. Curro, and K. S. Schweizer, J. Chem. Phys. **94**, 4659 (1991).
[4] J. M. Torkelson, Macromolecules **20**, 1860 (1987).
[5] L. P. Chang and H. Morawetz, Macromolecules **20**, 428 (1987).
[6] G. H. Fredrickson, Macromolecules **19**, 441 (1986).
[7] F. Mikes, H. Morawetz, and K. S. Dennis, Macromolecules **13**, 969 (1980).
[8] F. Amrani, J. M. Hung, and H. Morawetz, Macromolecules **13**, 649 (1980).
[9] P. G. deGennes, *Scaling Concepts in Polymer Physics* (Cornell University, Ithaca, NY, 1979).
[10] P. J. Flory, J. Macromol. Sci.-Phys. B **12**, 1 (1976).
[11] F. Boue, M. Daoud, M. Nierlich, C. Williams, J. P. Cotton, B. Farnoux, G. Jannink, H. Benoit, R. Dupplessix, and C. Picot, International Atomic Agency, Vienna, 1977, p. 563.
[12] O. F. Olaj and K. H. Pelinka, Makromol. Chem. **177**, 3413 (1976).
[13] P. G. deGennes, J. Phys. **31**, 235 (1970).
[14] P. J. Flory, *Principles of Polymer Chemistry* (Cornell University, Ithaca, NY, 1953).
[15] K. A. Peterson, M. B. Zimmt, S. Linse, R. P. Domingue, and M. D. Fayer, Macromolecules **20**, 168 (1987).
[16] M. D. Ediger, R. P. Domingue, K. A. Peterson, and M. D. Fayer, Macromolecules **18**, 1182 (1985).
[17] A. H. Marcus, Nathan A. Diachun, Deborah M. Hussey, and M. D. Fayer (unpublished).
[18] D. S. Kaplan, J. Appl. Polymer. Sci. **20**, 2615 (1976).
[19] K. U. Finger, A. H. Marcus, and M. D. Fayer, J. Chem. Phys. (in press).
[20] A. H. Marcus, N. A. Diachun, and M. D. Fayer, J. Phys. Chem. (in press).
[21] A. H. Marcus and M. D. Fayer, J. Chem. Phys. **94**, 5622 (1991).
[22] J. D. Byers, W. S. Parsons, R. A. Friesner, and S. E. Webber, Macromolecules **23**, 1789 (1990).
[23] K. A. Peterson, A. D. Stein, and M. D. Fayer, Macromolecules **23**, 111 (1990).
[24] I. Yamazaki, N. Tamai, and T. Yamazaki, J. Phys. Chem. **94**, 516 (1990).
[25] T. Forster, Ann. Phys. **2**, 55 (1948).
[26] T. Forster, Radiation Res. Suppl. **2**, 326 (1960).
[27] H. Friebolin, *Basic One- and Two-Dimensional NMR Spectroscopy* (VCH, New York, 1993).
[28] J. B. Birks, *Photophysics of Aromatic Molecules* (Wiley-Interscience, London, 1970).
[29] D. L. Huber, Phys. Rev. B **20**, 2307 (1979).
[30] D. L. Huber, Phys. Rev. B **20**, 5333 (1979).
[31] A. Blumen, J. Chem. Phys. **72**, 2632 (1980).
[32] J. Baumann and M. D. Fayer, J. Chem. Phys. **85**, 4087 (1986).
[33] S. W. Haan and R. J. Zwanzig, J. Chem. Phys. **68**, 1879 (1978).
[34] B. J. Berne and R. Pecora, *Dynamic Light Scattering* (Krieger, Malabar, FL, 1976).
[35] M. D. Ediger and M. D. Fayer, J. Chem. Phys. **78**, 2518 (1983).
[36] The initial forward transfer step in electron transfer processes follow DT kinetics. For simplicity, the present formulation is limited to excitation transfer processes. However, the reader should be aware that the model may be as easily applied to the forward step in electron transfer reactions.
[37] H. Yamakawa, *Modern Theory of Polymer Solutions* (Harper & Row, New York, 1971).
[38] K. G. Honnell, J. G. Curro, and K. S. Schweizer, Macromolecules **23**, 3496 (1990).
[39] K. S. Schweizer and J. G. Curro, J. Chem. Phys. **89**, 3350 (1988).
[40] K. S. Schweizer and J. G. Curro, J. Chem. Phys. **89**, 3342 (1988).
[41] K. S. Schweizer and J. G. Curro, Phys. Rev. Lett. **58**, 246 (1987).
[42] J. G. Curro and K. S. Schweizer, Macromolecules **20**, 1928 (1987).
[43] J. G. Curro and K. S. Schweizer, J. Chem. Phys. **87**, 1842 (1987).
[44] I. Ohmine, R. Silbey, and J. M. Deutch, Macromolecules **10**, 862 (1977).
[45] M. Doi and S. F. Edwards, *The Theory of Polymer Dynamics* (Oxford University, Oxford, 1986).

[46] J. P. Hansen and I. R. McDonald, *Theory of Simple Liquids*, 2nd ed. (Academic, New York, 1986).
[47] A. H. Narten, A. Habenschuss, K. G. Honnell, J. D. McCoy, J. G. Curro, and K. S. Schweizer, J. Chem. Soc. Faraday Trans. **88**, 1791 (1992).
[48] K. S. Schweizer, J. G. Curro, Chem. Phys. **149**, 105 (1990).
[49] D. V. O'Connor and D. Phillips, *Time-Correlated Single Photon Counting* (Academic, London, 1984).
[50] The data presented in Fig. 3 and reproduced from Ref. 1 has been numerically smoothed according to a block average algorithm.
[51] S. Phan, E. Kierlik, and M. L. Rosinberg, J. Chem. Phys. **99**, 5326 (1993).